

Learning Scheme Based on Stability Analysis for Prediction Model of Anesthetic Effect Using Recurrent Neural Network

¹Yoshitomo Sakuma, ²Kento Takabayashi, ³Takumi Kobayashi, ³Chika Sugimoto and ³Ryuji Kohno,

¹Graduate School of Science and Engineering, Yokohama National University, Yokohama, Japan.

²Faculty of Computer Science and System Engineering, Okayama Prefectural University, Okayama, Japan;

³Faculty of Engineering, Yokohama National University, Yokohama, Japan.

Abstract—This paper proposes a learning scheme for the Recurrent Neural Network (RNN) model to predict the anesthetic effect on a patient during surgery to support stable controlling anesthesia in clinical operation under lack of anesthesiologists. The goal of this study is to realize dependable control of total intravenous anesthesia (TIVA) to support anesthesiologists. To realize dependable control of anesthesia, it is necessary to satisfy various restrictions to guarantee safety on anesthesia and the use of model predictive control (MPC) is effective in controlling anesthesia to meet those requirements. In the MPC, the stability of the prediction model is very important to guarantee the control performance. Also, the RNN is useful for modeling nonlinear systems with time variations, such as patient drug response. Although stability of an existing learning scheme using the RNN has not been analyzed, the paper investigates the stability of the proposed learning scheme using the RNN by a manner of Lyapunov analysis.

Keywords—Prediction Model, Total Intravenous Anesthesia, Machine Learning, Recurrent Neural Network, Stability Analysis

I. INTRODUCTION

The application of machine learning (ML) and data science to the medical field attracts much attention due to the increase in the aging population and a shortage of medical staff [1–3]. In particular, the shortage of medical staff (e.g., anesthesiologists) presents major problem [4,5]. The shortage of anesthesiologists may lead to poor management of the patient’s anesthesia and an increased risk of postoperative sequelae. To ameliorate this problem and to ensure the safety of surgical operations, dosage control systems for total intravenous anesthesia (TIVA) have been proposed [6,7]. In general, administration of anesthesia requires appropriate sedation, analgesia, and muscle relaxation to ensure patient safety [8]. For example, physiological information indicating anesthetic effects and dose restriction of propofol [9] for sedation should be taken into account. The bispectral index (BIS) [10] is often used as an index of anesthetic depth. Table 1 shows the relationship between the BIS value and the patients’ condition. Hence, it shows that the desired BIS value during surgery ranges from 40 to 60.

Although a control scheme for a TIVA using model predictive control (MPC) was proposed [11–16] considering those requirements, it has not taken into account of time variance of BIS.

Then, scientific researchers have proposed the estimation scheme of time variance of BIS using a parametric model [17,18] and extended Karman filter (EKF) [19,20]. The parametric model was built with the assumption that drug

absorption in a human body is limited to four fluid compartments.

TABLE I. BJSPECTRALINDEX [10]

Condition of the patients	Value of BIS
Awaken	From 90 to 100
Light Hypnosis	From 60 to 90
Desired range	From 40 to 60
Deep Hypnosis	From 0 to 40

Although the relationship between drug concentration in a human body and drug effect assumed to be estimated by nonlinear equation [18], the full picture of the action mechanism of the anesthetic drug is much more complicated. There are more hidden factors like degradation of the liver function through alcoholic liver disease [21] or stimulations to the patients by the treatment during surgery [15,16].

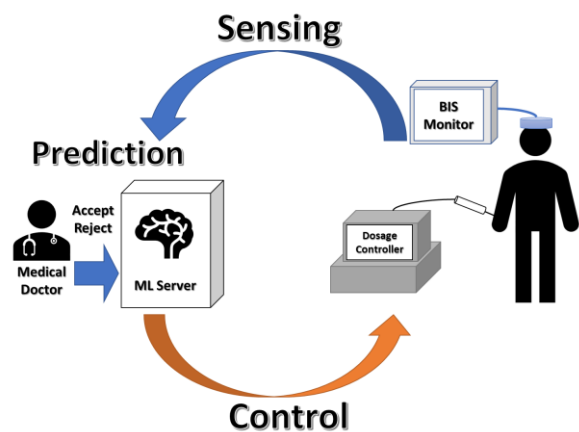


Fig. 1. The conceptual diagram of the proposal

To improve performance of TIVA using MPC by taking care of recurrent but time-variant non-linear factors of human body response corresponding to anesthetic dosage, we propose an on-line feedback sensing and controlling loop system for TIVA as illustrated its concept in Fig. 1. The proposed system can model or estimate human body response, that is time transition of BIS value, corresponding to anesthetic dosage with recurrent neural network (RNN) [22]. And to catch up time variance of body condition, the proposed system applies stochastic gradient descent (SGD) with a backpropagation algorithm as an on-line learning rule [23].

The feedback loop procedure of learning with RNN using sensed BIS values and controlling anesthetic dosage is described as follows:

- Step 1:**The BIS monitor measures the current BIS value of the patient.
- Step 2:**The BIS monitor sends the current BIS value to the ML server.
- Step 3:**The ML server updates the RNN model using the current BIS value with following SGD algorithm.
- Step 4:**The ML server calculates the optimum dosage volume by the prediction using RNN model.
- Step 5:**If the anesthesiologist accepted the calculated optimum dosage volume, The ML server sends the control command (the optimum dosage volume) to the infusion pump. Otherwise, the anesthesiologist decides the dosage.
- Step 6:**The dosage controller controls the infusion pump based on the received command.
- Step 7:**Back to the Step 1 and repeat the Step 1-6 until the surgery operation is finished.

This paper investigates stability of the proposed scheme learned by SGD dependent on the learning rate to update the network parameters and optimization of the learning rate while our previous study [22] was not taken into account of the stability. Moreover, although other scientific researchers proposed an estimation scheme of time transition of drug effects using neural networks [24], the stability of those schemes were not discussed. Hence, this paper proposes learning the prediction model using the RNN to predict the anesthetic effect considering the network stability.

The main contribution and novelty of the manuscript are as follows:

1. The stability of the RNN is analyzed using a manner of Lyapunov analysis [25]. From the analysis, the condition of the stability and optimum learning rate for each parameter in the RNN model are derived. Furthermore, the manuscript proposes the system which can improve adaptability and identification speed faster within a condition of stability.
2. Novel performance evaluations considering various patient, which were not considered in our previous work [22]. From the evaluation, the efficiency of our proposed scheme is confirmed.

The rest of this paper is organized as follows. In Section 2, the system model and our proposed scheme is explained. In Section 3, the theoretical analysis of the learning stability is performed and the optimum learning rate is discussed. In Section 4, performance evaluations using numerical simulations is explained. In Section 5, discussion of the simulation results is described. Finally, Section 6 concludes our work and discuss future works.

II. SYSTEM MODEL

In this section, the procedure of our proposed system is described in detail.

A. Structure of Our Proposed System

Fig. 2 shows the diagram of our proposed system. The aim of the system is to predict an anesthetic effect and optimize drug dosages based on the prediction. In this paper, the estimation aspect of the system is focused, in which drug dosages $u[t]$ are optimized in each time t . The prediction is based on BIS estimator using recurrent neural network (RNN) model. Moreover, the network parameters were updated using training data, $y[t]$ (normalized BIS value sensed from the patient). The normalization of the BIS value is calculated as follows:

$$y[t] = \frac{BIS[t]}{E_0} \quad (1)$$

where, E_0 is BIS when the anesthetic drug is administrated to the patient. We assumed the value to be measured before surgery.

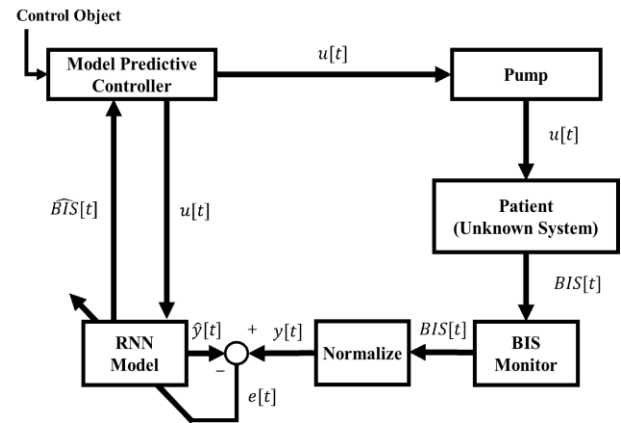


Fig. 2. The block diagram of the proposed system

In next subsection, the composition of the RNN model and the estimation scheme of the BIS behavior are explained.

B. Recurrent Neural Network Model

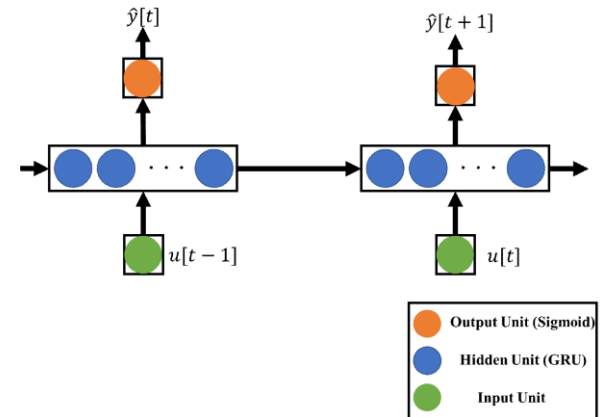


Fig. 3. RNN model

In this subsection, an RNN model for predicting the BIS behavior is described. Fig. 3 shows the structure of the RNN. In our proposed system drug dosages in each time $u[t]$ served as input to the RNN. In the hidden layer, it is assumed that the time variance of the drug absorption in the human body is expressed as the feature of nodes. In order to express the time variance of drug effect in human body, gated re current units (GRU) mechanism [26] is applied. The GRU is one of the gating mechanisms to compose the RNN. It can express the effect of previous feature to current feature. The composition of the GRU is expressed as follows:

$$\begin{aligned} z_i[t] &= \sigma(w_{1,i}[t]u[t] + \mathbf{w}_4[t]^T \mathbf{h}[t-1]) \\ r_i[t] &= \sigma(w_{2,i}[t]u[t] + \mathbf{w}_5[t]^T \mathbf{h}[t-1]) \\ h_i[t] &= (1 - z_i[t])h_i[t-1] + z_i[t]\hat{h}_i[t] \\ \hat{h}_i[t] &= \tanh(w_{3,i}[t]u[t] + \mathbf{w}_6[t]^T (r_i[t] \circ \mathbf{h}[t-1])), \quad (2) \end{aligned}$$

where \circ denotes the Hadamard product operator, and $z_i[t]$ and $r_i[t]$ denote the factors to control effects of previous features in the hidden layers. Those factors can be expressed as vectors: $\mathbf{z}[t] = [z_1[t], z_2[t], \dots, z_N[t]]^T$ and

$\mathbf{r}[t] = [r_1[t], r_2[t], \dots, r_N[t]]^T$ where, N denotes number of the GRU units in hidden layer. $w_{1,i}[t]$, $w_{2,i}[t]$, and $w_{3,i}[t]$ are weight parameters for input $u[t]$ which can be expressed as vectors: $\mathbf{w}_i[t] = [w_{i,1}[t], w_{i,2}[t], \dots, w_{i,N}[t]]^T$ ($i = 1, 2, 3$). Also, \mathbf{w}_4 , \mathbf{w}_5 , and \mathbf{w}_6 denotes the weight vectors to outputs of the hidden layers $\mathbf{h}[t] = [h_1[t], h_2[t], \dots, h_N[t]]^T$. $\sigma(x)$ denotes sigmoid function:

$$\sigma(x) = \frac{1}{1 + e^{-x}} \quad (3)$$

Fig. 4 shows the composition of GRU units.

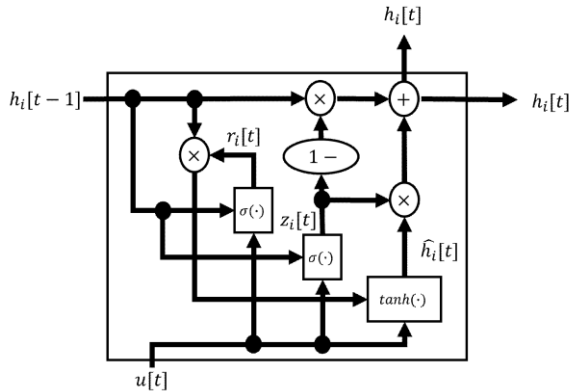


Fig. 4. Gated Recurrent Units [26]

Notice that i is the index number of the GRU units. These weight parameters were updated in our RNN model by the learning algorithm.

In addition, the estimated value of the normalized BIS $\hat{y}[t]$ were expressed in the output layer. The value ranges 0 to 1, and it assumed to be nonlinear. Thus, the sigmoid function is applied as an activation function of the output layer and output of the RNN model expressed as follows:

$$\hat{y}[t] = \frac{1}{1 + e^{-\mathbf{w}_7[t]^T \mathbf{h}[t]}} \quad (4)$$

In equation (4), $\mathbf{w}_7[t]$ denotes weight vector of the output layer. Finally, by using measured maximum value of BIS E_0 , the estimated BIS value $\widehat{BIS}[t]$ can be expressed as follows:

$$\widehat{BIS}[t] = E_0 \hat{y}[t]. \quad (5)$$

C. Prediction Algorithm of BIS Value

Fig. 5 shows the flowchart of our proposed system. The t_{end} denotes the end time of the surgery period. In this flowchart, the BIS value is sensed from patients and used to update RNN model in each time step and converted to training data of the RNN prediction model $y[t]$ through normalization. Using the training data $y[t]$ in each time step, weights in the RNN model are updated by stochastic gradient descent (SGD) [23] algorithm. In the SGD algorithm, the weights of the Neural Network are updated to minimize the value of evaluation function. The evaluation function $E[t]$ in each time step is defined as square error between the training data $y[t]$ (Normalized BIS) and the output of the RNN model $\hat{y}[t]$ in order to minimize the prediction error of BIS value. Hence, the function $E[t]$ is defined as follows:

$$E[t] = \frac{1}{2} (y[t] - \hat{y}[t])^2. \quad (6)$$

Using the evaluate function in (6), weights $w_{i,j}$ ($i = 1, 2, \dots, 7, j = 1, 2, \dots, N$) are updated as follows:

$$w_{i,j}[t+1] = w_{i,j}[t] - \mu_{i,j} \frac{\partial E[t]}{\partial w_{i,j}[t]} \quad (7)$$

where, $\mu_{i,j}$ denotes learning rate for each weight, and $\frac{\partial E[t]}{\partial w_{i,j}[t]}$

is partial derivative of $E[t]$ with respect to $w_{i,j}[t]$. Based on (7), weights $w_{i,j}[t]$ are updated sequentially to minimize evaluate function $E[t]$ while the learning of the RNN model proceeds. However, learning performance depends on the value of the learning rate μ . When the learning rate μ is too small, the speed to improve the estimation accuracy by the RNN becomes slow. When the learning rate μ is too large, convergence stability and estimation accuracy using the RNN model cannot be guaranteed. Therefore, we analyzed the stability of learning theoretically and derived the optimum learning rate μ based on the analysis. In the next section, the stability analysis is described in detail.

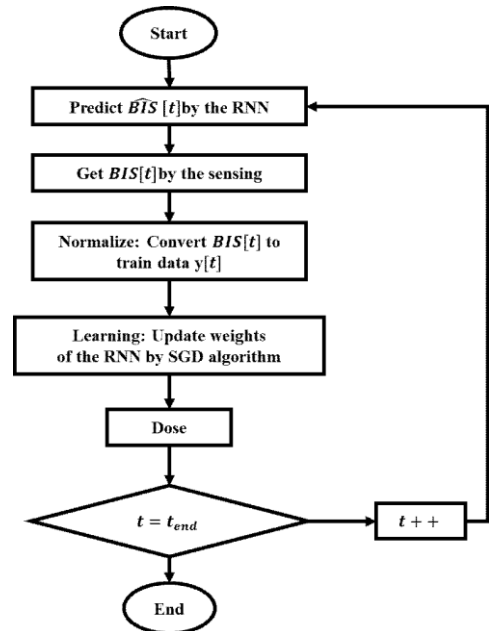


Fig. 5. Flowchart of the proposed scheme

III. STABILITY ANALYSIS AND OPTIMIZATION OF THE LEARNING RATE

In this section, the stability of the learning algorithm is analyzed based on Lyapunov analysis [25]. The Lyapunov analysis is used to analyze the stability of systems based on the Lyapunov function $L(t)$. From the Lyapunov's stability theorem, if the time derivative of Lyapunov function $\dot{L}(t)$ takes negative value, the system became stable. In the discrete-time system, the differential of Lyapunov function $\Delta L[t] = L[t+1] - L[t]$ is used to analyze the stability. Also, the squared error between the system output and the desired signal can be applied as the Lyapunov function. Thus, we applied Lyapunov function $E[t]$ for the stability analysis in our RNN model. The error between training data $y[t]$ and the output of the RNN model $\hat{y}[t]$ are expressed as:

$$e[t] = y[t] - \hat{y}[t]. \quad (8)$$

The Lyapunov function $L[t]$ can be expressed as

$$L[t] = \frac{1}{2} (e[t])^2. \quad (9)$$

From (8) and (9), time differential of Lyapunov function $\Delta L[t] = L[t+1] - L[t]$ can be expressed as

$$\begin{aligned}
\Delta L[t] &= L[t+1] - L[t] \\
&= \frac{1}{2} \{(e[t+1])^2 - (e[t])^2\} \\
&= \frac{1}{2} \{(e[t] + \Delta e[t])^2 - (e[t])^2\} \\
&= \Delta e[t] \left(e[t] + \frac{1}{2} \Delta e[t] \right) \quad (10)
\end{aligned}$$

Where $\Delta e[t] = e[t+1] - e[t]$ denotes the differential of error in each time step. Using partial derivative $\frac{\partial e[t]}{\partial w_{i,j}[t]}$ and (7), $\Delta e[t]$ can be also expressed as

$$\begin{aligned}
\Delta e[t] &= \sum_{i=1}^7 \sum_{j=1}^N \left(\frac{\partial e[t]}{\partial w_{i,j}[t]} \right) (w_{i,j}[t+1] - w_{i,j}[t]) \\
&= \sum_{i=1}^7 \sum_{j=1}^N \left(\frac{\partial e[t]}{\partial w_{i,j}[t]} \right) \left(w_{i,j}[t] - \mu_{i,j} \frac{\partial E[t]}{\partial w_{i,j}[t]} - w_{i,j}[t] \right) \\
&= - \sum_{i=1}^7 \sum_{j=1}^N \mu_{i,j} \left(\frac{\partial e[t]}{\partial w_{i,j}[t]} \right) \left(\frac{\partial E[t]}{\partial w_{i,j}[t]} \right). \quad (11)
\end{aligned}$$

Here, the relationship between partial differential $\frac{\partial E[t]}{\partial w_{i,j}[t]}$ and $\frac{\partial e[t]}{\partial w_{i,j}[t]}$ can be expressed as

$$\frac{\partial E[t]}{\partial w_{i,j}[t]} = e[t] \frac{\partial e[t]}{\partial w_{i,j}[t]}. \quad (12)$$

From (11) and (12), supposing $e[t] \neq 0$, the differential $\Delta e[t]$ can be re-written as

$$\begin{aligned}
\Delta e[t] &= - \sum_{i=1}^7 \sum_{j=1}^N \frac{\mu_{i,j}}{e[t]} \left(\frac{\partial E[t]}{\partial w_{i,j}[t]} \right)^2 \\
&= - \frac{1}{e[t]} \mathbf{q}^T \boldsymbol{\mu} \quad (13)
\end{aligned}$$

where $\mathbf{q} = [q_{1,1}, q_{1,2}, \dots, q_{1,N}, q_{2,1}, \dots, q_{7,N}]^T$, $q_{i,j} = \left(\frac{\partial E[t]}{\partial w_{i,j}[t]} \right)^2$, and $\boldsymbol{\mu} = [\mu_{1,1}, \mu_{1,2}, \dots, \mu_{1,N}, \mu_{2,1}, \dots, \mu_{7,N}]^T$ respectively. From (13) and (10), the differential of the Lyapunov function $\Delta L[t] = L[t+1] - L[t]$ can be re-written as

$$\begin{aligned}
\Delta L[t] &= - \frac{1}{e[t]} \mathbf{q}^T \boldsymbol{\mu} \left(e[t] - \frac{1}{2} \frac{1}{e[t]} \mathbf{q}^T \boldsymbol{\mu} \right) \\
&= - \frac{1}{(e[t])^2} \mathbf{q}^T \boldsymbol{\mu} \left((e[t])^2 - \frac{1}{2} \mathbf{q}^T \boldsymbol{\mu} \right) \\
&= \frac{1}{4E[t]} \mathbf{q}^T \boldsymbol{\mu} (\mathbf{q}^T \boldsymbol{\mu} - 4E[t]). \quad (14)
\end{aligned}$$

Therefore, from (14), the condition to guarantee stability of the RNN can be expressed as

$$0 \leq \mathbf{q}^T \boldsymbol{\mu} \leq 4E[t]. \quad (15)$$

Here, (14) can be transformed to

$$\Delta L[t] = \frac{1}{4E[t]} \boldsymbol{\mu}^T \mathbf{Q} \boldsymbol{\mu} - \mathbf{q}^T \boldsymbol{\mu}. \quad (16)$$

where $\mathbf{Q} = \mathbf{q} \mathbf{q}^T$. Preventing from decreasing speed of the evaluation function, $\Delta L[t]$ is desired to minimize in each time

step. Then, solving the formula $\frac{\partial \Delta L[t]}{\partial \mu} = 0$ using (16), the optimum learning rate μ^* can be expressed as follows:

$$\mu^* = 2E[t] \mathbf{Q}^{-1} \mathbf{q}. \quad (17)$$

In this paper, we updated learning rate μ adaptively based on (17).

IV. PERFORMANCE EVALUATION AND DISCUSSIONS

A. Condition of Evaluations

In this section, some evaluations to confirm the prediction accuracy of our proposal are performed. Thus, the BIS behaviors of 12 patients are simulated to evaluate the efficiency of our proposal. To simulate the true BIS value for each patient, the *Schnider* and *Minto* model [17] was applied. Also, the parameter sets used in [12] were applied as the simulation parameter of each 12 patients.

TABLE II. SIMULATION PARAMETERS

Simulation time [min.]	70
Sampling Period T_s [sec.]	5
Gain of the PID controller	
Proportional Gain: K_p ,	0.055,
Integral Gain: K_i ,	0.001
Derivative Gain: K_d	2.68
Target BIS value in the control	50
Learning rate in the conventional	0.50, 1.00, 5.00
Number of GRU in hidden layer N (the size of weight vectors)	9
Number of hidden layers	1

Table 2 shows the simulation parameters. In the simulation, it is assumed that the sampling period of the BIS value from the BIS monitor to be 5.0 second, which is the same as the BIS monitor used in [10]. The dosages in each time step were controlled by the a PID control with a target BIS value of 50. The gain of the PID controller was decided based on Ziegler-Nichols' method [27] that is one of the typical methods to decide the gain. Furthermore, to evaluate the efficiency of our proposed system compared the prediction performance of our proposed system that of the conventional scheme. The conventional scheme used fixed learning rate to update its network parameters.

We evaluated the estimated BIS value, the absolute error between estimated BIS value, and the true BIS value. The mean absolute error (MAE) during surgery which denotes the average of absolute error over a period of time was also evaluated. The MAE is defined as follows:

$$MAE = \frac{1}{T} \sum_{t=1}^T |BIS[t] - \widehat{BIS}[t]| \quad (18)$$

where, T denotes the number of samples. Also, in the simulation, we defined allowable absolute error as 7.5 considering, taking into account the target BIS value (50.0) and the desired range with margin (42.5 and 57.5) [10].

B. Simulation Results and Discussions

Here, the simulation results in the introduction period is described. The MAE of this period is shown in Table 3. The MAE values in the proposal are lower than that of conventional in all patients. For example, in evaluation of Patient 10, the

MAE value in the proposal takes 0.05, and that is the lowest value in the simulation.

TABLE III. RESULT OF THE MEAN ABSOLUTE ERROR

Patient ID	Proposal	$\mu=0.50$	$\mu=1.00$	$\mu=5.00$
1	0.09	0.57	0.36	5.36
2	0.11	0.79	0.55	5.33
3	0.09	0.75	0.52	0.24
4	0.11	0.29	0.17	4.63
5	0.08	0.43	0.27	1.23
6	0.08	0.59	0.41	0.18
7	0.07	0.44	0.28	0.11
8	0.1	0.41	0.28	0.17
9	0.12	0.49	0.34	0.18
10	0.05	0.44	0.29	0.12
11	0.06	0.24	0.14	0.07
12	0.07	0.4	0.24	3.39

Fig. 6 shows the transition of the BIS value of the Patient 10. From Fig. 6, it can be seen that the estimated BIS value from the proposed scheme (i.e., the blue line) is closer to the true value (i.e., the dotted line) than that of the conventional scheme. On the other hand, the estimated BIS values by all conventional seem to be closed slower to the true value compared to the proposal. Fig. 7 shows the absolute error between the estimated BIS value by the RNN model and the true value.

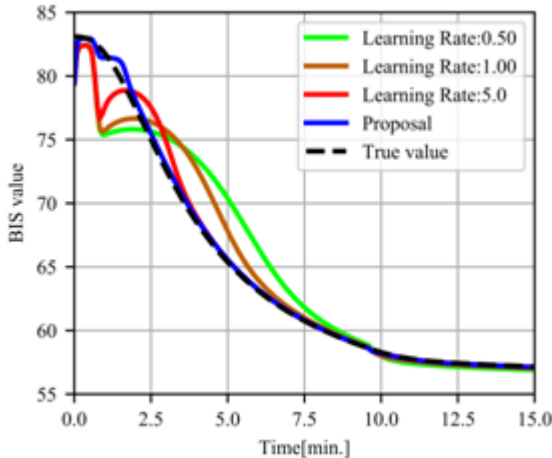


Fig. 6. Transition of the BIS value in the Patient 10

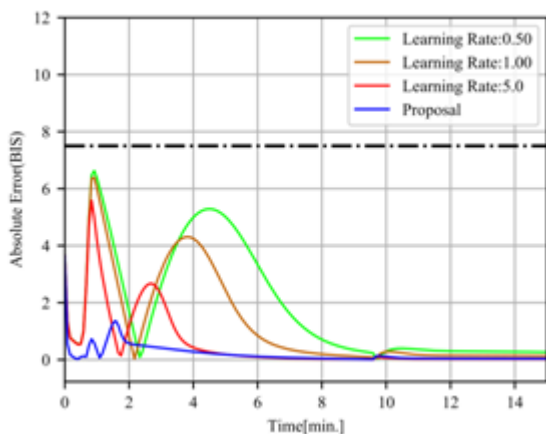


Fig. 7. Transition of absolute error in the Patient 10

From Fig. 7, we confirmed that the absolute error in the proposal (i.e., the blue line) always takes lower than 4.0. The maximum absolute error in the all conventional higher than that of our proposal. In particular, in the case learning rate is fixed to 5.00, the value of absolute error takes higher than 6.0 and that closes to the allowable error in the simulation (i.e., broken line). From those results, we confirmed that the efficiency of our proposed scheme was superior to the scheme with a fixed learning rate.

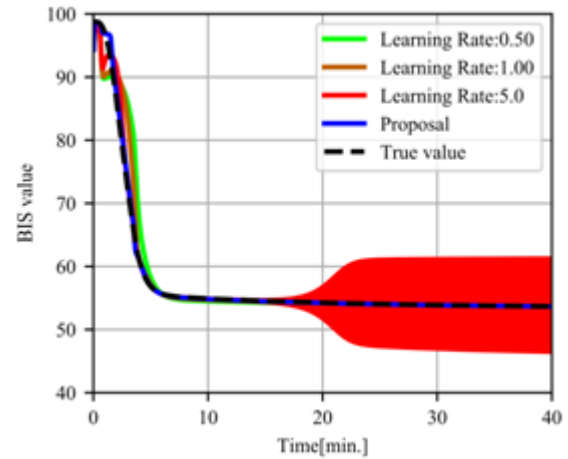


Fig. 8. Transition of the BIS value in the Patient 1

Next, from Table 3, in the case that learning rate is fixed to 5.00, we confirmed that the MAE takes 5.36 in the evaluation in Patient 1. It is the highest value of all the patients. Fig. 8 shows the transition of the BIS value of the Patient 1. From Fig. 8, the estimated BIS value by the proposed scheme (i.e., the blue line) seems to be closer to the true value (i.e., the dotted line) than that of the conventional scheme. Also, we confirmed that the estimated BIS value when the learning rate is fixed to 5.00 began to oscillate from about 20 minutes.

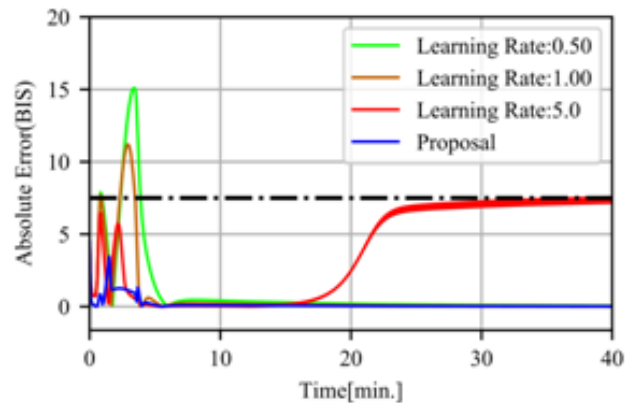


Fig. 9. Transition of absolute error in the Patient 1

Fig. 9 shows the absolute error between the estimated BIS value of the RNN model and true value. From Fig. 9, we confirmed that the absolute error in the proposal (i.e., the blue line) always takes less than 5.00, while the maximum absolute error in the all conventional takes higher than allowable absolute error in the simulation (i.e., broken line). Also, in the case that learning rate is fixed to 5.00, we confirmed that the absolute error become higher from about 20 minutes. From those results, we confirmed that our proposed scheme demonstrated higher performance compared to the conventional scheme. Especially, we confirmed that optimization of the learning rate can prevent unstable state of the outputs of the RNN.

CONCLUSION

This paper proposes a learning scheme for the prediction model of the anesthetic drug effect using RNN with GRU. Thus, the stability of the RNN model is analyzed using Lyapunov analysis, and the optimum learning rate for each parameter of the RNN model is derived. The prediction performance of our proposed scheme is compared to the conventional scheme with a fixed learning rate by the computer simulation. From the numerical result, it is confirmed that our proposed scheme achieves higher prediction performance than the conventional scheme.

As for the future research, the effective control scheme of anesthesia using the RNN model learned with our proposed scheme should be considered. In addition, whether our proposed scheme can be applied to similar applications should be considered, for example, the application to predict the effect of insulin for Diabetes.

References

- [1] Mothkur, R.; Poornima, K.M. Machine Learning will Transfigure Medical Sector: A Survey. 2018 International Conference on Current Trends towards Converging Technologies (ICCTCT), 2018, pp. 1–8. doi:10.1109/ICCTCT.2018.8551134.
- [2] SUZUKI, K. Survey of Deep Learning Applications to Medical Image Analysis. *Medical Imaging Technology* 2017, 35, 212–226. doi:10.11409/mit.35.212.
- [3] Shah, P.; Kendall, F.; Khozin, S.; Goosen, R.; Hu, J.; Laramie, J.; Ringel, M.; Schork, N. Artificial intelligence and machine learning in clinical development: a translational perspective. *NPJ digital medicine* 2019, 2, 1–5. doi:https://doi.org/10.1038/s41746-019-0148-3.
- [4] Takeda, J. Measures to address the manpower shortage in anesthesiology in Japan. *JAPAN MEDICAL ASSOCIATION JOURNAL* 2007, 50, 325.
- [5] Miller, R.D.; Lanier, W.L. The Shortage of Anesthesiologists: An Unwelcome Lesson for Other Medical Specialties. *Mayo Clinic Proceedings* 2001, 76, 969 – 970. doi:https://doi.org/10.4065/76.10.969.
- [6] Alexander, R.; Volpe, N.G. Total Intravenous Anesthesia. *Anaesthesia, Pain, Intensive Care and Emergency Medicine— A.P.I.C.E.*; Gullo, A., Ed.; Springer Milan: Milano, 2002; pp. 819–823.
- [7] Paz, L.A.; Silva, M.M.; Esteves, S.; Rabico, R.; Mendonca, T. Automated total intravenous anesthesia (amTIVA) from induction to recovery. 2014 IEEE International Symposium on Medical Measurements and Applications (MeMeA), 2014, pp. 1–6. doi:10.1109/MeMeA.2014.6860039.
- [8] Park, G.R. Sedation, analgesia and muscle relaxation and the critically ill patient. *Canadian Journal of Anaesthesia* 1997, 44, R40–R51. doi:10.1007/BF03022264.
- [9] Scott, R.; Saunders, D.; Norman, J. Propofol: clinical strategies for preventing the pain of injection. *Anaesthesia* 1988, 43, 492–494. doi:10.1111/j.1365-2044.1988.tb06641.x.
- [10] Ontario, H.Q.; others. Bispectral index monitor: an evidence-based analysis. *Ont Health Technol Assess Ser* 2004, 4, 1–70.
- [11] Sakuma, Y.; Sameshima, K.; Kohno, R. An adaptive scheme of controlling dosage and dosing interval in general anesthesia by model predictive control using anesthetic depth model. 2017 11th International Symposium on Medical Information and Communication Technology (ISMICT), 2017, pp. 77–81. doi:10.1109/ISMICT.2017.7891772.
- [12] Nascu, I.; Krieger, A.; Ionescu, C.M.; Pistikopoulos, E.N. Advanced Model-Based Control Studies for the Induction and Maintenance of Intravenous Anaesthesia. *IEEE Transactions on Biomedical Engineering* 2015, 62, 832–841. doi:10.1109/TBME.2014.2365726.
- [13] Savoca, A.; Barazzetta, J.; Pesenti, G.; Manca, D. Model predictive control for automated anesthesia. In 28th European Symposium on Computer Aided Process Engineering; Friedl, A.; Klemeš, J.J.; Radl, S.; Varbanov, P.S.; Wallek, T., Eds.; Elsevier, 2018; Vol. 43, Computer Aided Chemical Engineering, pp. 1631 – 1636. doi:https://doi.org/10.1016/B978-0-444-64235-6.50284-9.
- [14] Krieger, A.; Pistikopoulos, E.N. Model predictive control of anesthesia under uncertainty. *Computers & Chemical Engineering* 2014, 71, 699 – 707. doi:https://doi.org/10.1016/j.compchemeng.2014.07.025.
- [15] Ingole, D.D.; Sonawane, D.N.; Naik, V.V.; Ginoya, D.L.; Patki, V. Implementation of Model Predictive Control for Closed Loop Control of Anesthesia. *Mobile Communication and Power Engineering*; Das, V.V.; Chaba, Y., Eds.; Springer Berlin Heidelberg: Berlin, Heidelberg, 2013; pp. 242–248.
- [16] Nascu, I.; Pistikopoulos, E.N. A multiparametric model-based optimization and control approach to anaesthesia. *The Canadian Journal of Chemical Engineering* 2016, 94, 2125–2137. doi:10.1002/cjce.22634.
- [17] Schneider, Thomas W., D.M.; Minto, Charles F., M.C.; Gambus, Pedro L., M.; Andresen, Corina, M.; Goodale, David B., D.P.; Shafer, Steven L., M.; Youngs, Elizabeth J., M. The Influence of Method of Administration and Covariates on the Pharmacokinetics of Propofol in Adult Volunteers. *Anesthesiology: The Journal of the American Society of Anesthesiologists* 1998, 88, 1170–1182.
- [18] Sawaguchi, Y.; Furutani, E.; Shirakami, G.; Araki, M.; Fukuda, K. A Model-Predictive Hypnosis Control System Under Total Intravenous Anesthesia. *IEEE Transactions on Biomedical Engineering* 2008, 55, 874–887. doi:10.1109/TBME.2008.915670.
- [19] Rezvani, S.; Towhidkhalah, F.; Ghahramani, N.; Rezvani, A. Increasing Robustness of the Anesthesia Process from Difference Patient's Delay Using a State-Space Model Predictive Controller. *Procedia Engineering* 2011, 15, 928 – 932. CEIS 2011, doi:https://doi.org/10.1016/j.proeng.2011.08.171.
- [20] Rezvani, S.; Towhidkhalah, F.; Ghahramani, N. Controlling the depth of anesthesia using model predictive controller and Extended Kalman Filter. 2011 1st Middle East Conference on Biomedical Engineering, 2011, pp. 213–216. doi:10.1109/MECBME.2011.5752103.
- [21] Vaja, R.; McNicol, L.; Sisley, I. Anaesthesia for patients with liver disease. *Continuing Education in Anaesthesia Critical Care & Pain* 2009, 10, 15–19. doi:10.1093/bjaceaccp/mkp040.
- [22] Sakuma, Y.; Kohno, R. A Dynamic Model Estimation Scheme for Model Predictive Control of Anesthesia Using Recurrent Neural Network. 2018 12th International Symposium on Medical Information and Communication Technology (ISMICT), 2018, pp. 1–5. doi:10.1109/ISMICT.2018.8573720.
- [23] Bottou, L. Online learning and stochastic approximations. *On-line learning in neural networks* 1998, 17, 142.
- [24] Ali, J.B.; Hamdi, T.; Fnaiech, N.; Costanzo, V.D.; Fnaiech, F.; Ginoux, J.M. Continuous blood glucose level prediction of Type 1 Diabetes based on Artificial Neural Network. *Biocybernetics and Biomedical Engineering* 2018, 38, 828 – 840. doi:https://doi.org/10.1016/j.bbe.2018.06.005
- [25] LYAPUNOV, A.M. The general problem of the stability of motion. *International Journal of Control* 1992, 55, 531–534. doi:10.1080/00207179208934253.
- [26] Cho, K.; van Merriënboer, B.; Gülçehre, Ç.; Bougares, F.; Schwenk, H.; Bengio, Y. Learning Phrase Representations using RNN Encoder-Decoder for Statistical Machine Translation. *CoRR* 2014, abs/1406.1078, [1406.1078].
- [27] Ziegler, J. G., and Nichols, N. B. (June 1, 1993). "Optimum Settings for Automatic Controllers." *ASME. J. Dyn. Sys., Meas., Control*. June 1993; 115(2B): 220–222. https://doi.org/10.1115/1.2